The Effect of Reverted Austenite on the Mechanical Properties and Toughness of 12 Ni and 18 Ni (200) Maraging Steels

C. A. PAMPILLO AND H. W. PAXTON

A study has been made of the effects of reverted austenite on the mechanical properties and toughness of three maraging steels. It is found that reverted austenite has no detrimental effects on the mechanical properties and toughness and even improves these properties when precipitated along martensite lath boundaries. This occurs for underaged specimens. A detrimental effect on toughness is found when reverted austenite precipitates at prior austenitic grain boundaries which occurs for overaged specimens. Overaged precipitates are also responsible for the decrease in toughness in the overaged condition.

THE effects of reverted austenite on the mechanical properties and toughness of maraging steels is somewhat contradictory in the literature. It has been stated[1] that although reverted austenite may improve fabricability if introduced at an intermediate stage of processing, it should be eliminated by cold work or reannealing. However, Floreen[2] has suggested that the presence of austenite in 18 Ni (250) maraging steel could explain its higher toughness relative to other grades of maraging steels when compared at equal strengths.[3-4] This could be connected to Legendre's finding[5] showing that the uniform elongation of tensile samples of a 19 Ni 9 Co 5 Mo maraging steel increased substantially when the steel was heat treated so that some reverted austenite was produced. The connection is made through the correlation which seems to exist between uniform elongation and fracture toughness.[6-7] We would like to report here some results on the effect of reverted austenite on the mechanical properties and toughness of two 12 Ni, 5 Cr, 3 Mo (J and A) and a 18 Ni, 8 Co, 3 Mo (200 grade) (K) maraging steel.

MATERIALS AND EXPERIMENTAL PROCEDURE

The two 12 Ni steels differed in melting practice producing a different distribution of inclusions, presumably not changed further by the subsequent heat treatments. Steel J is from a vacuum induction melt, and steel A from an electric furnace melt. Steel K was melted by vacuum induction. The composition of the three steels is shown in Table I.

All aging treatments were performed after austenitizing for 2 h at 850°C and oil quenching. Optical micrographs showed inclusions 5 to 10 μ in size in the three steels. In steels J and K the distance between inclusions is approximately 150 to 300 μ and in steel A between 50 and 100 μ.

The load-elongation curves of the steels (after different aging times at 565° and 520°C) were obtained from cyclindrical tensile specimens 0.8 in. in gage length and 0.185 in. in diameter at a strain rate of 0.1 min^{-1}.

The amount of reverted austenite formed after different times at the different aging temperatures, was measured by comparing the X-ray integrated intensities of (211) α with the mean values of the integrated intensities of (311) γ and (220) γ; these two last peaks should be equal if no texture is present. This averaging minimizes the errors due to the mild texture actually present[8] (the difference in integrated intensities of the (311)γ and the (220)γ was less than 30 pct). The radiation used was molybdenum filtered with zirconium, which due to the relative insensitivity of the absorption coefficients to the different elements present in the steels, minimized errors due to changes in composition of the phases at the different aging times. No corrections were made for the fact that a third phase was present, *i.e.* the precipitates. This leads to an overestimation of the amount of austenite present by some few percent at the longest aging times.[9]

The room temperature toughness of the different microstructures was determined on fatigue-precracked Charpy specimens broken by impact. The energy spent in breaking unit fracture area of the specimen was

Table I. Composition of Steels

Steel	A	J	K
Ni	11.12	11.75	18.10
Mo	3.16	3.04	3.09
Co	0.09	0.09	8.55
Cr	4.80	4.74	0.015
Ti	0.25	0.23	0.23
Al	0.042	0.068	0.092
Mn	0.08	0.064	0.047
Si	0.089	0.050	0.065
C	0.020	0.012	0.011
P	0.005	0.011	0.005

C. A. PAMPILLO, formerly with the Department of Metallurgy and Materials Science, Carnegie-Mellon University, Pittsburgh, Pa., is now Research Physicist, Materials Research Center, Allied Chemical Corporation, Morristown, N. J. 07960. H. W. PAXTON, on leave from Carnegie-Mellon University, is Director, Division of Materials Research, National Science Foundation, Washington, D. C.

Manuscript submitted August 27, 1971.

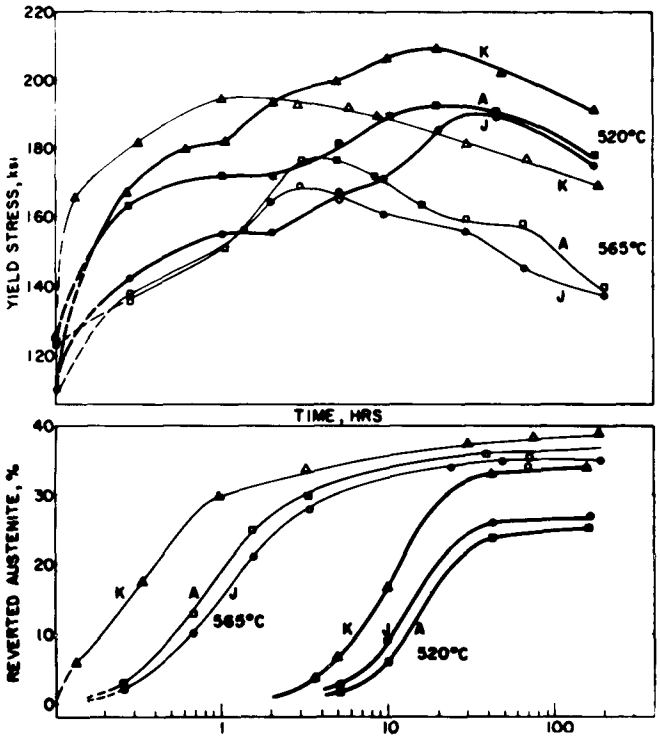

Fig. 1—Yield stress and volume fraction of reverted austenite as a function of aging time.

taken as a measure of the toughness of the material. Plane strain conditions are by no means present in the specimens, and the energies obtained should not be taken as a measure of G_{IC}, *i.e.* the plane-strain crack resistance force. The reported values are the mean values of at least three specimens.

The fracture surfaces were examined by two stage plastic-carbon replicas. Thin films for transmission electron microscopy observation were prepared by using a 10 pct perchloric acid in acetic acid solution as electrolyte in a jet polishing unit.

RESULTS

Mechanical Properties

Fig. 1 shows the yield stress of the three steels as a function of aging time at 565° and 520°C. In the same graph, we have plotted the amount of reverted austenite as a function of aging time at 520° and 565°C. The amount of austenite increases rapidly at the beginning of the reaction; eventually the rate decreases sharply and a plateau is reached.

It is interesting to note that at both temperatures and for all three steels the sharp change in the rate of formation of austenite occurs at the same time the peak yield stress is reached. At this point, 28, 30, and 30 pct austenite formed at 565°C is present in the J, A, and K steels respectively; meanwhile, 25, 22, and 29 pct austenite were formed at 520°C. The amounts reached after 198 h at 565°C are 35, 37 and 39 pct and at 520°C after 160 h 26, 25, and 34 pct respectively. This shows that the decrease of the yield stress found after the peak has been reached probably is not due entirely to reversion of austenite but also to overaging of the hardening precipitates. The amount of austenite at the peak yield stress is substantially greater than

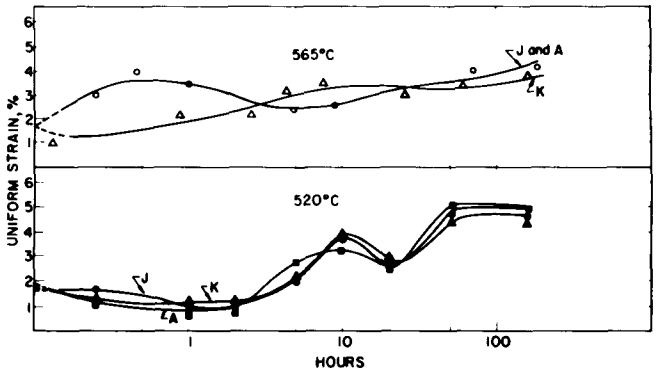

Fig. 2—Uniform plastic strain as a function of aging time.

the value of 14 pct found by Peters for Fe-18 Ni-Mo age-hardenable alloys, at peak hardness[9] after aging at 482°C.

At 565°C, both precipitation (observed with the electron microscope) and the reversion of martensite to austenite seem to occur simultaneously. At 520°C, however, some precipitation raises the yield stress by about 50 ksi for the J and A steels and 70 ksi for the K steel before the reversion of martensite to austenite starts. Just before austenite is detected in all three steels the yield stress remains constant for a certain aging time perhaps due to some dissolution of the precipitates. Thereafter, the yield stress continues to increase by about 34, 20, and 28 ksi for the J, A, and K steels respectively even though the amount of reverted austenite increases rapidly. The same is observed at 565°C from the beginning of aging; interestingly enough then, the presence of reverted austenite thought to be a weak phase does not seem to reduce the yield stress and even may be increasing it. The uniform strain was found to increase with aging time. At 565°C for the A and J steels, the uniform strain increases rapidly with aging time from a value of ~1.3 pct for the unaged specimens to about 4 pct after aging for 0.25 h. A slight decrease in elongation is found around the peak yield stress and finally, an increase to about 5.2 pct for the longer aging times (150 h). For steel K the trend is similar although the first rapid increase is slower; the uniform strain increases from 1.3 pct to about 2.5 pct after 1 h aging, and to about 4 pct at the longer aging times (150 h). At 520°C where precipitation starts much before austenite reversion, uniform elongation did not increase until austenite started to form. This is seen in Fig. 2 which shows how the uniform strain varies with aging time at 520° and 565°C. A slight decrease in the uniform strain at small aging times is found, followed by a rapid increase when austenite starts to form. A modest drop in the uniform strain is found at peak yield stress, followed by a rise presumably associated with the overaging of precipitates. Some of the load elongation curves, measured after different times, at 520°C are shown in Fig. 3 for steel J; the numbers on each curve are the aging times in hours. Similar curves were found for steel A and K.

Toughness*

*Note that from the method of measurement, this is only a relative term.

Fig. 4 shows the values of fracture energy found for

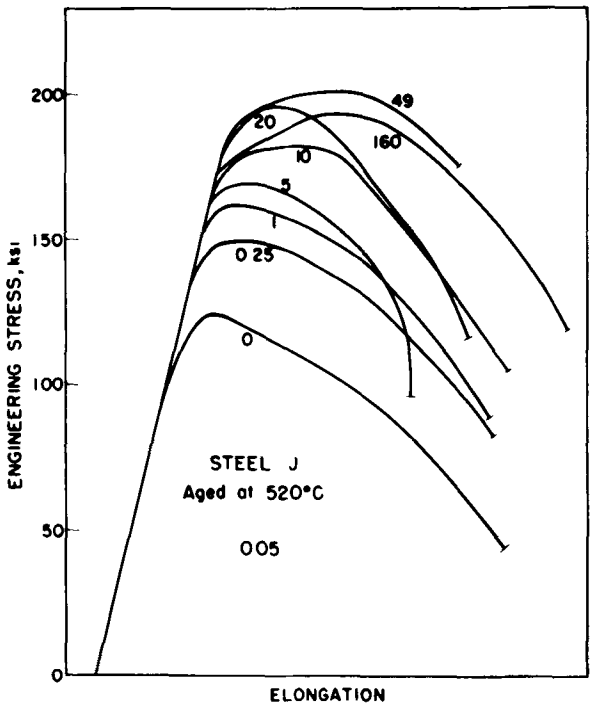

Fig. 3—Load elongation curves after different aging times at 520°C for steel J.

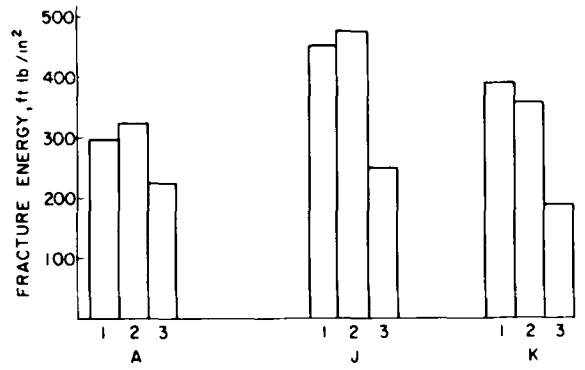

Fig. 4—Fracture energy for three microstructures of each steel.

each steel in three different conditions but at the same yield stress. This is illustrated schematically in Fig. 5. The three microstructures which are discussed in the following section are:

1) essentially no reverted austenite with some precipitation hardening
2) some reverted austenite and underaged precipitates
3) some reverted austenite and overaged precipitates

The 12 Ni steels were tested at a yield stress of 160 ksi and the 18 Ni steel at 180 ksi. For the three steels, there is no important difference in toughness between the microstructures 1 and 2. However, the microstructure 3, *i.e.*, the overaged condition, shows a lower toughness in all three steels. It is interesting to note that in the overaged condition both steels A and J show the same toughness although steel J is tougher than A when in the underaged conditions 1 and 2. Moreover, the toughness of steel K at a yield stress of 180 ksi is higher than that of steel A at 160 ksi.

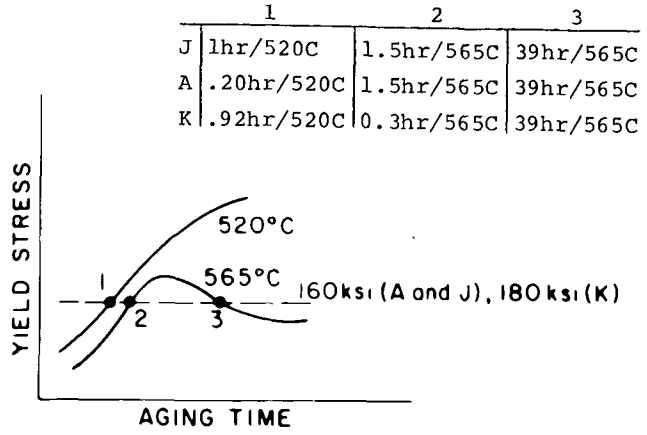

Fig. 5—Illustrating schematically microstructures 1, 2, and 3 on the yield stress aging time plot.

Microstructure

Fig. 6(*a*), (*b*) and (*c*) shows optical micrographs of the three microstructures 1, 2, and 3, respectively, of steel A. Although the microstructure 2 has about 25 pct of reverted austenite, this is not recognizable on the micrographs. The difference in appearance between microstructure 1 with no austenite and microstructure 2 is mainly that the latter one seems to show finer microstructure. When in the overaged condition, however, the austenite is readily seen as white ribbons, possibly due to changes in composition which make the etchant more effective. The ribbons of austenite seem to be interspersed within the grains and in some cases exist at prior austenitic grain boundaries, as seen in Fig. 6(*d*) for steel K. Figs. 7(*a*), (*b*), and (*c*) show transmission electron micrographs of steel J after aging for a) 0.25 h and b) 1 h at 565°C.

After aging for 0.25 h at 565°C, the micrographs show a high density of dislocations on which precipitates have formed. These precipitates have been identified by Leo[10] as possibly Ni_3Ti, or Fe_2Ti, but are definitely not Ni_3Mo which seems to be the primary strengthening precipitate in the 18 Ni (250) grade (2).

After aging for 0.25 h at 565°C, about 3 pct reverted austenite is indicated at room temperature from X-ray measurements. The austenite seems to nucleate at martensite lath boundaries forming a film about 0.05 μ thick. The same has been reported for 18 Ni (250) maraging steel[11] and for Fe-Ni binary massive martensites.[12]

At longer times (1 h) the precipitates have grown and are easily seen as elongated rods or plates 0.3 μ long by 0.03 μ thick, Fig. 7(*b*). This is the microstructure we have called 2 and from the fractographs, it appears these particles are not contributing significantly to form voids during the fracture process.

At times of the order 9 h the yield stress of the material has dropped about 5 pct from peak yield stress. At this point precipitates have grown but are not much larger than those shown for microstructure 2. After 72 h, the appearance is somewhat similar. These particles do, however, contribute during the fracture process to the nucleation of voids, as we have seen in the fractographs. It seems likely then that the easier nucleation of voids at particles in the overaged con-

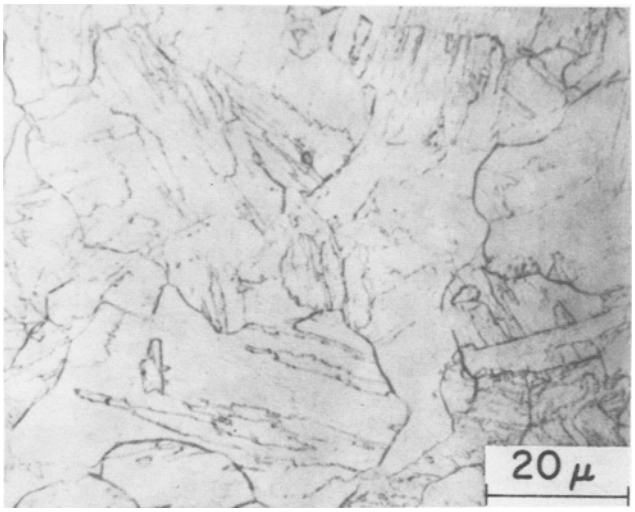

(a)

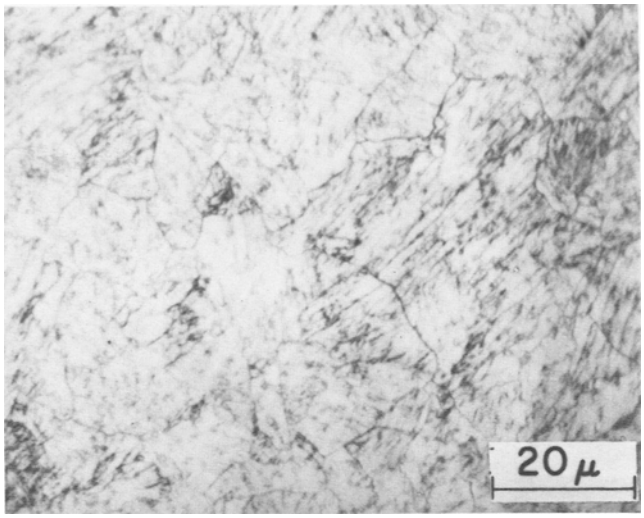

(b)

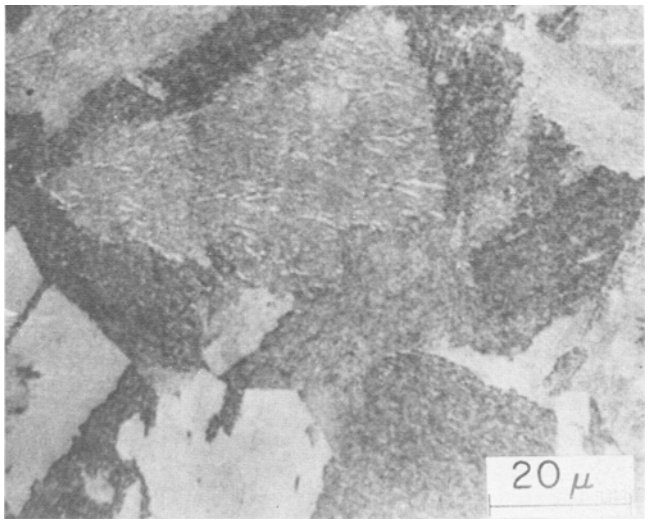

(c)

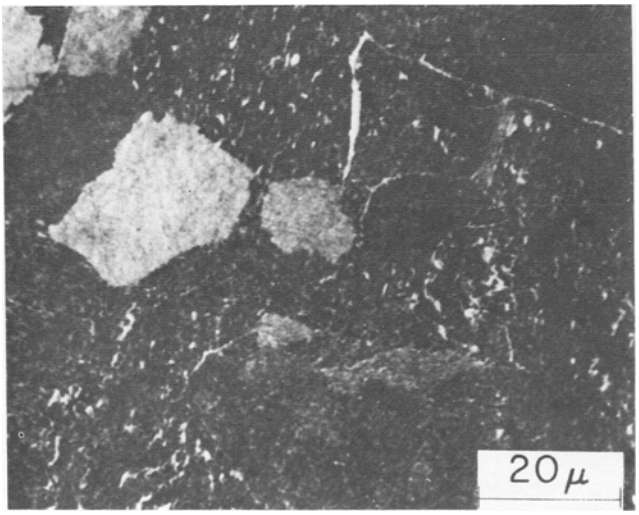

(d)

Fig. 6—Optical micrographs of microstructures: 1 at (*a*) (0.2 h at 520°C) 2 at (*b*) (1.5 h at 565°C) and 3 at (*c*) (39 h at 565°C) for steel A and microstructure 3 at (*d*) for steel K (39 h at 565°C).

dition may be due to loss of coherency and perhaps weakening of the particle interface.

The prior austenitic grain boundaries seem to be free of precipitates; however, the optical micrographs show some reverted austenite can form at these boundaries. Figs. 8(*a*) and (*b*) show electron micrographs of steel J aged at 520°C, 1 hr at (*a*) and for 5 h at (*b*). It is possible to see that for the 5 h age, austenite has formed at the lath boundaries.

Fractography

Two stage plastic-carbon replicas of the fracture surfaces of the steels were made. Figs. 9 and 10 show the fracture topography of steel J with the microstructures 1 and 3 respectively. The one corresponding to the microstructure 2 shows similar topography to that in 1. Steels A and K show somewhat similar features. Structures 1 and 2 contain large dimples of the order of 10 to 20 μ in diameter. From their distribution and number it is possible to state that not all of these dimples have been nucleated at the large inclusions seen with the optical microscope. Either the hardening precipitates or impurity particles, too fine to see in the optical microscope, must have nucleated some of these large dimples.

In the lower toughness, overaged condition, a few large dimples are found, but in general there is a high density of very small (0.5 to 1 μ) dimples. These small dimples have very probably been nucleated at overaged particles.

DISCUSSION

Our data on toughness and tensile properties shows that reverted austenite does not have deleterious effects for aging times smaller than the peak stress aging time, *i.e.* in the underaged condition. We shall first discuss the tensile properties.

As mentioned earlier, in all three steels at 520°C the initiation of the reversion reaction is anticipated by an interruption in the increase of the yield stress with aging time. This may mean that, at this point, some dissolution of precipitates has occurred. It is

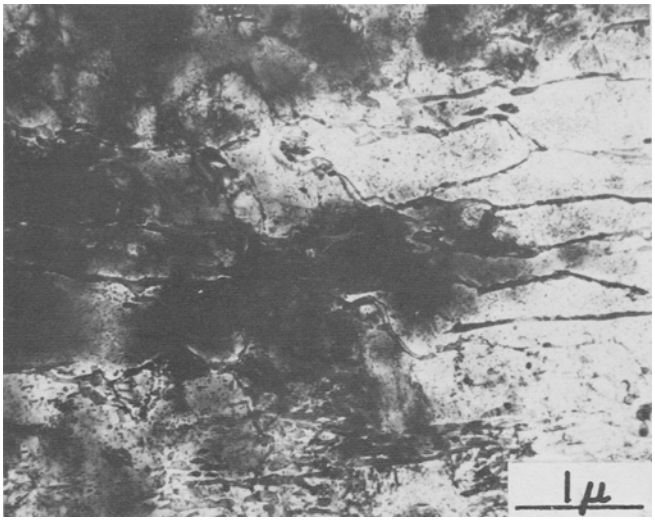

(a)

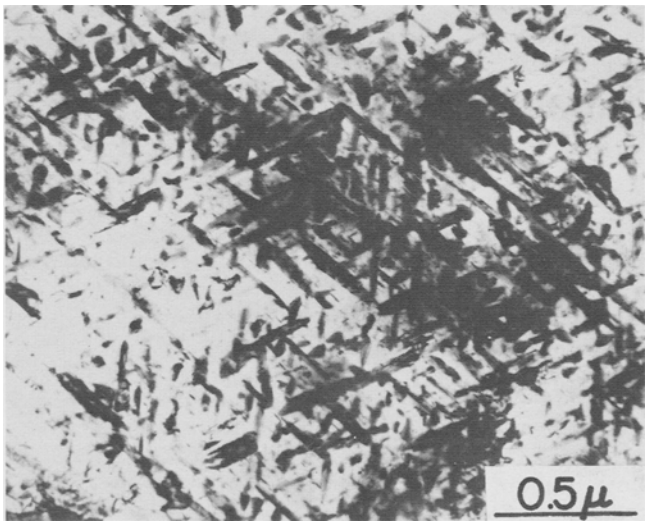

(b)

Fig. 7—Transmission electron micrographs of steel J after aging for 0.25 h at 565°C at (*a*) and 1 h at 565°C at (*b*) (microstructure 2).

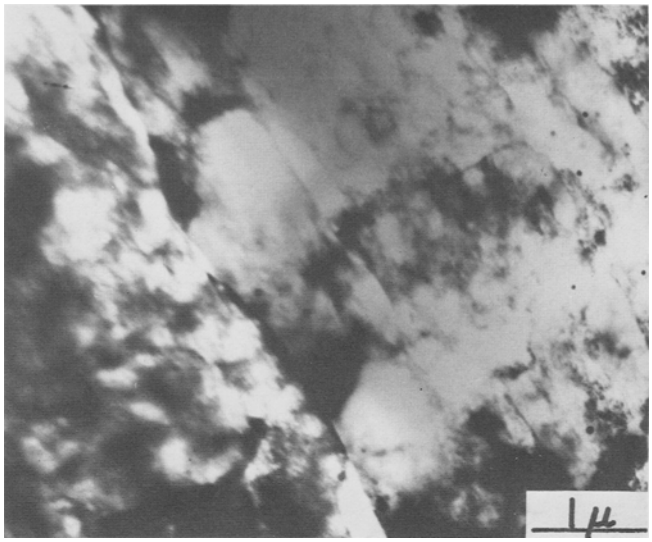

(a)

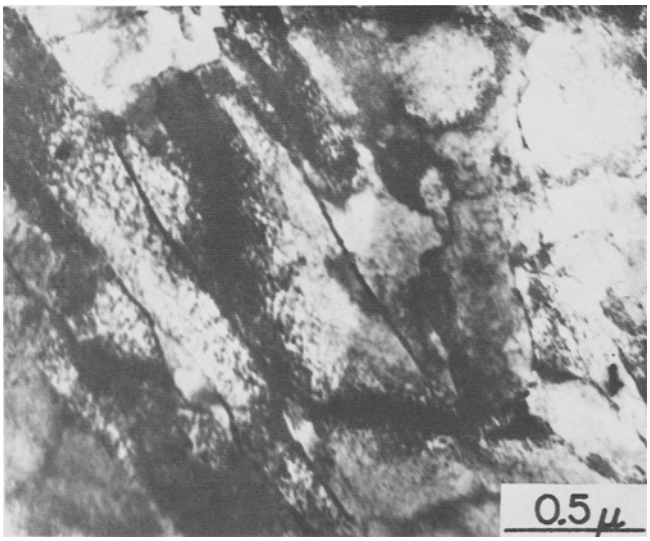

(b)

Fig. 8—Transmission electron micrographs of steel J aged at 520°C for 1 h at (*a*) (microstructure 1) and for 5 h at (*b*).

tempting, then, to suggest that the dissolution of the hardening precipitates initiates the austenite reversion reaction. This has been suggested previously for other maraging compositions[9] where the dissolution of Ni_3Mo and precipitation of Fe_2Mo should produce a local enrichment of the matrix in austenite stabilizers. The same is likely to happen if Ni_3Ti dissolves and Fe_2Ti is formed. With the X-ray technique for measuring reverted austenite, it is difficult to estimate exactly when austenite does start to form and therefore to show unequivocally that this occurs after the interruption in the increase in yield stress with aging time. The yield stress of the steels is not reduced by the introduction of reverted austenite (a softer phase). In fact, at both temperatures the yield stress increases in parallel with the increase in reverted austenite and starts to decrease when the amount of austenite almost has reached a plateau. The fact that austenite forms at the martensite lath boundaries suggests the possibility of a positive contribution of austenite to the yield stress. This may be analyzed through the possible effects on the ability of the martensite lath boundaries to act as slip barriers. We should point out first, that the orientation relationship between adjacent laths leads to low angle type boundaries.[13] These boundaries are not supposed to be effective as obstacles to slip. The known effect of prior austenitic grain size on the yield stress of massive martensites[15] indicates just this. When forming at the martensite lath boundaries, austenite should contribute to increasing the difficulty of transmitting slip across these boundaries. This could be due to a relaxation of stress concentration at the head of dislocations piled up against the boundaries, caused by the austenite, or to a more efficient dislocation grain boundary source provided by the austenite martensite boundaries (which should be of a high angle type), as follows from Li's model for grain boundary strengthening.[14]

The values found for the uniform strains are quite small especially in the unaged condition. Fig. 2, par-

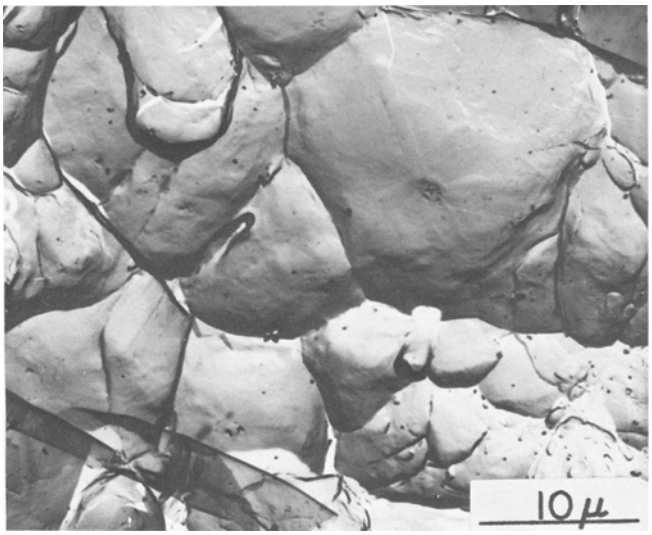

Fig. 9—Two-stage plastic carbon replica of the fracture surface of steel J with microstructure 1 (1 h at 520°C).

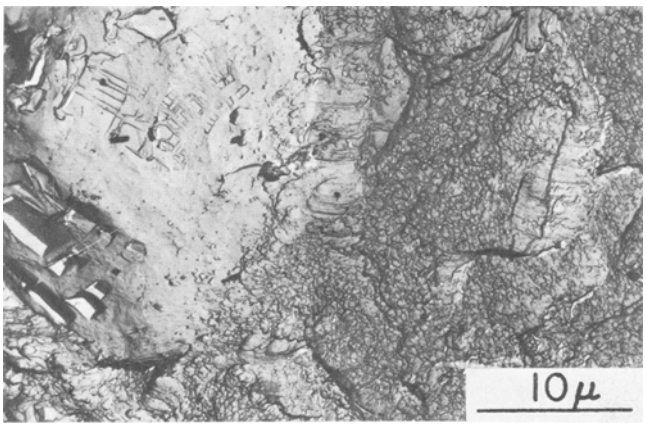

Fig. 10—Two-stage plastic carbon replica of the fracture surface of steel J with microstructure 3 (39 h at 565°C).

ticularly for the 520°C aging, suggests that reverted austenite increases the uniform strain by a factor of 2 or 3. We first turn to the question of why is the uniform strain in the unaged martensite so small. In a tensile specimen, necking starts when the rate of work hardening is equal to the flow stress. The amount of deformation necessary to reach this situation may depend on the type of strengthening mechanism, how fast dynamic recovery is reached and so on. Mechanisms which increase the yield stress without increasing the hardening rate should lead to smaller uniform strains. Such may be the case of grain boundary strengthening for which it is found that for grain sizes smaller than about 10 μ the uniform strain decreases sharply.[16] However, as we have already pointed out before, there is a measurable effect of the prior austenite grain size on the yield stress[15] which means that this is the grain size to take into account (20 to 40 μ). We believe that the small uniform strains are due to the dislocation structure introduced during the martensitic transformation. Floreen,[2] prompted by some experiments made by Basinski and Jackson in copper single crystals[17] has suggested that the "alien" distribution of

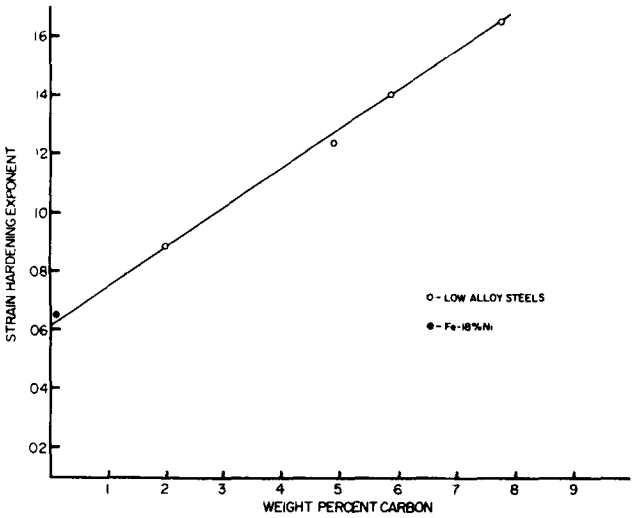

Fig. 11—Effect of carbon on strain hardening exponent at flow stress of 80 kg/sq mm (from Ref. 15).

dislocations introduced during the martensitic transformation may be responsible for the propensity of slip to be concentrated in localized bands in a 18 pct Ni-Fe binary alloy.[15] We would like to suggest here that this "alien" distribution of dislocations may be responsible for the small uniform strains reported here. Such a distribution may contribute to increase the yield stress but because it may be unstable to slip[17] leads to a decrease in the strain hardening and hence the small uniform strains. In this connection, it seems interesting to recall the observations made by Hollomon[18] on the dependence on carbon concentration of the hardening exponent n in the expression $\sigma = K\epsilon^n$ for the stress-strain curves of low alloy steels. The steels followed such an expression and the value of n was therefore equal to the uniform strain. Fig. 11 shows Hollomon's data replotted by Floreen.[15] The hardening exponent or uniform strain is found to increase markedly with the concentration of carbon. The value of n at almost zero carbon concentration is that of an 18 pct Ni-Fe binary alloy[15] (it is not stated in Ref. 15 if this is equal to the uniform strain). The effect of carbon on the uniform strain of low alloy steels seems to be in agreement with the above discussion for it is expected that carbon will stabilize (through pinning of dislocations) the "alien distribution" introduced during the martensitic transformation, at least for carbon concentrations which are low enough for some tempering to occur during quenching.

As mentioned already, reverted austenite increases the uniform strain. When austenite starts to form, the uniform strain increases from a value of about 1 pct to approximately 4 pct after aging for 10 h. Two factors should be involved in this. One is due to the austenite itself. The other, in accordance with the previous discussion, results from the stabilization of the "alien distribution" of dislocations introduced by the martensitic transformation; this is probably due to precipitation on dislocations and redistribution during aging. Accordingly, the uniform strain should increase up to a value typical of a material with a very small grain size[16] for now, due to the reverted austenite, the martensite lath size (1 to 2 μ) should be the effective grain size.

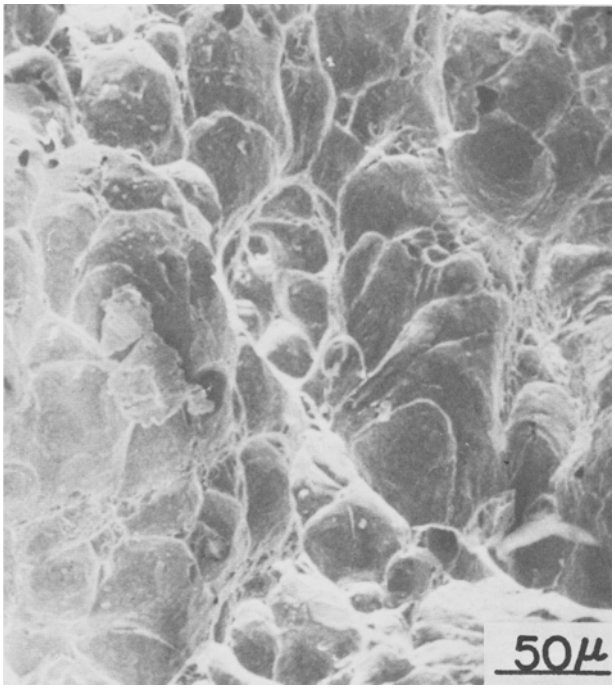

(a)

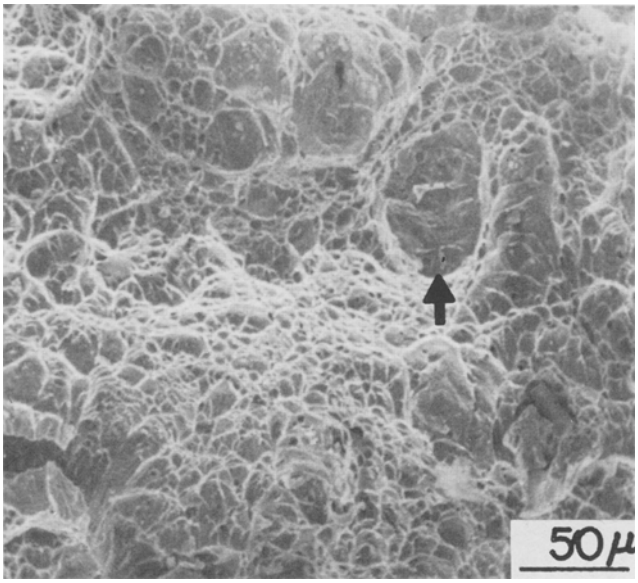

(b)

Fig. 12—Scanning electron micrographs of the fracture surface of steel K with microstructure 1 at (*a*) (0.92 h at 520°C) and 2 at (*b*) (0.3 h at 565°C).

We now turn to the effect on toughness. The results show that the effect of reverted austenite on toughness is small. So far observations of the fracture surface with either replicas in the transmission electron microscope or direct observation in the scanning electron microscope did not disclose any information to explain this in either steel J or A. In steel K, however, the scanning electron micrograph shown in Fig. 12 indicates that a larger number of smaller dimples appear in the microstructure 2 than that in 1. This suggests that a larger number of particles are nucleating voids. Since the different aging treatments do not change the distribution pattern of the large inclusions, the smaller voids must have been nucleated elsewhere, (very probably at hardening precipitates, possibly at reverted austenite).

It is interesting to note in Fig. 12 the presence of large dimples nucleated at large inclusions (shown by arrow). In spite of the fact that the material where this void has been formed contained particles able to nucleate small voids, the area covered by a large dimple is free from the smaller ones. The same may be seen in Fig. 10. This means that the nucleation of a void at a large inclusion and its subsequent growth relaxes the triaxiality necessary for growth of a void nucleated at smaller particles. The situation is very similar to that leading to the formation of the "stretched zone" at the beginning of unstable crack growth where a certain portion of the initial crack growth or blunting of the crack tip is produced without dimple formation because of the low triaxiality existing at that point.[19] The size of the dimple, in general several times the size of the inclusion, is then not directly due to the larger size of the inclusion but very likely to the earlier nucleation of voids at larger particles.

In the overaged microstructure, replicas showed very small dimples which could be associated with the overaged precipitates able to nucleate voids during the fracture process. The increased number of void nucleating sites was thought to be responsible for the much lower toughness of the steels possessing this microstructure. However, this explanation seems to be too simple because further observations show the existence of some prior austenitic grain boundary failures during fracture. This is shown in Fig. 13 for steels J and K. These micrographs were taken from Charpy specimens fractured by impact short of total failure. They were subsequently cut through the middle plane, perpendicular to the plane of the main fracture, polished and etched with 5 pct Nital. The reverted austenite precipitated at the prior austenitic grain boundaries could lead to this type of fracture path. This is possible if austenite forms a thin continuous film which is softer than the rest of the material. Excessive plastic deformation of this film will lead to early void nucleation and growth at the prior austenitic grain boundaries.[20] So far we have not been able to identify on replicas or by direct observation with the scanning electron microscope, areas of the fracture associated with austenitic grain boundaries.

CONCLUSIONS

1) Reverted austenite has no detrimental effect on the mechanical properties of 12 Ni and 18 Ni (200) maraging steels. In fact, it improves substantially its uniform elongation and may be responsible for part of the increase of yield stress with aging time.

2) This improvement and the fact that the yield stress increases with aging time along with the increase in the volume fraction of reverted austenite is believed to be due to the precipitation of austenite at the martensite lath boundaries.

3) In the underaged condition, *i.e.* before peak yield stress is reached, reverted austenite may improve toughness slightly.

4) In the overaged condition, reverted austenite

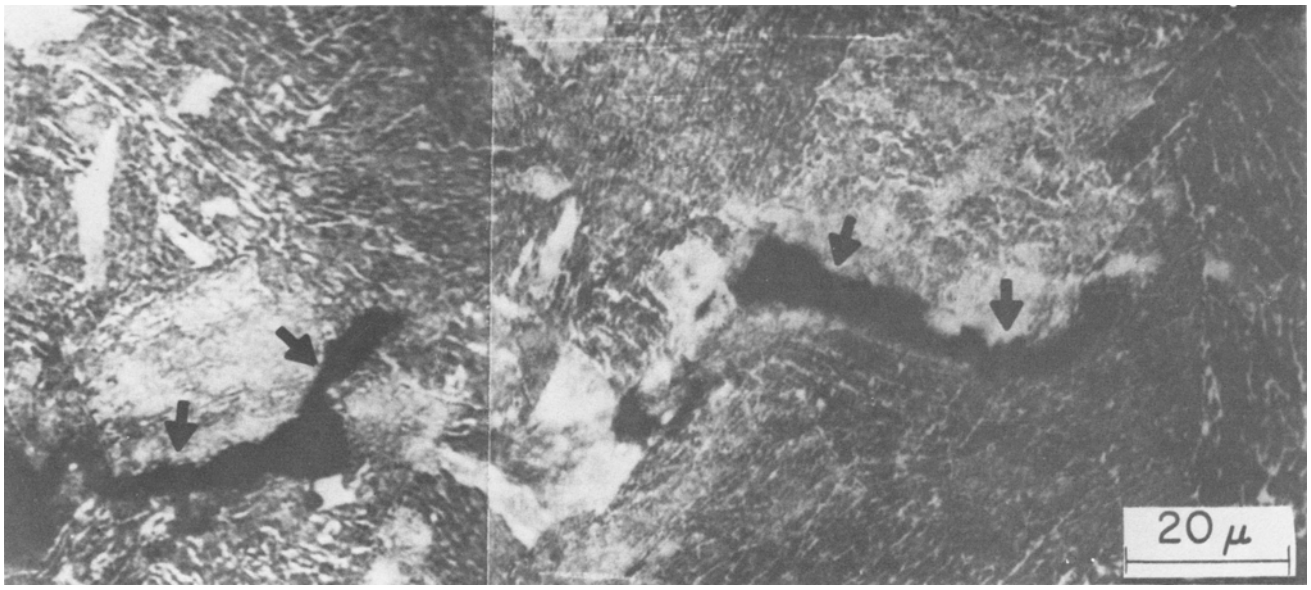

(a)

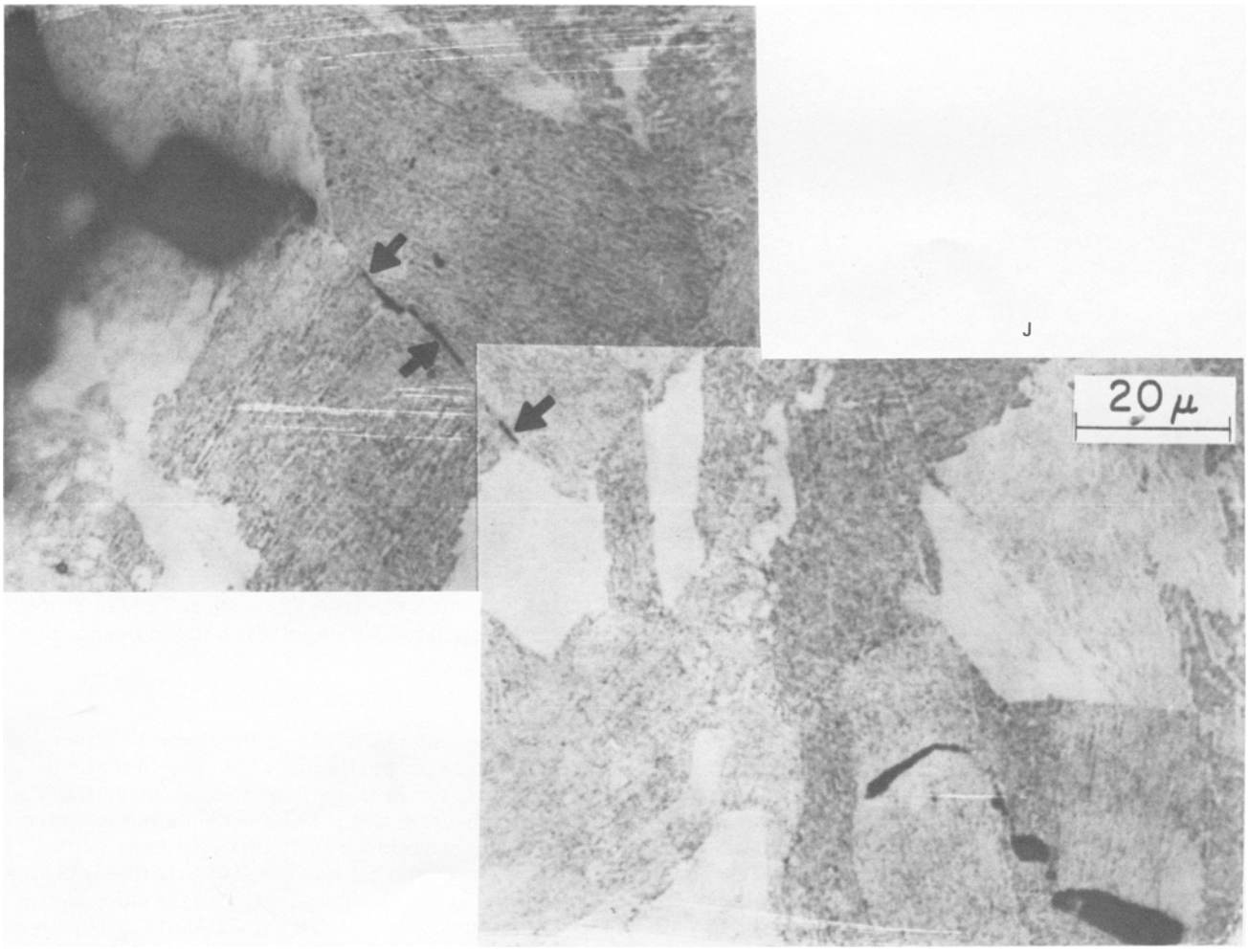

(b)

Fig. 13—Crack in a Charpy specimen of steel J and K with microstructure 3 (39 h at 565°C) showing some prior austenitic grain boundary failure shown by arrows. The main crack is on the left. Nital etch.

precipitates at prior austenitic grain boundaries and reduces toughness. Overaged precipitates which act as nuclei for void formation also play an important role in decreasing toughness.

5) The low uniform strains found for the three steels are considered to be due to the "alien distribution" of dislocations introduced during the martensitic transformation.

ACKNOWLEDGMENTS

We would like to thank Professor J. R. Low, Jr. for his encouragement and many valuable suggestions and stimulating discussions throughout this work. C. Freed of the Naval Research Laboratory, Washington, D.C., kindly provided the steels used in this study. Thanks are due to R. Miller, from the Edgar C. Bain Laboratory of United States Steel Corporation, for his help in the X-ray measurements which were made at that laboratory, and for many discussions. The help of Willis Poling in the electron microscopy is also appreciated.

This publication was made possible through a research grant of the Office of Naval Research.

REFERENCES

1. R. F. Decker, C. J. Novak, and T. W. Landing: *J. Metals,* November, 1967, p. 60.
2. S. Floreen: *Met. Rev.*, 1968, vol. 13, p. 115.
3. S. Floreen: *Trans. ASM,* 1964, vol. 57, p. 38.
4. S. Floreen and G. R. Speich *Trans ASM,* 1964, vol. 57, p. 714.
5. P. Legendre: *Cobalt,* 1965, vol. 29, p. 171.
6. J. M. Krafft: *Appl. Mater. Res.* 1964, vol. 3, p. 88.
7. G. T. Hahn and A. R. Rosenfield: *Amer. Soc. Testing Mater.* Spec. Tech. Publ. No. 432, 1968.
8. R. L. Miller: *Trans. ASM,* 1964, vol. 57, p. 892.
9. D. T. Peters: *Trans. ASM,* 1968, vol. 61, p. 62.
10. W. Leo: unpublished research, Carnegie-Mellon University, Pittsburgh, Pa.
11. S. Floreen and R. F. Decker: *Trans. ASM,* 1962, vol. 55, p. 518.
12. G. R. Speich: *Trans. TMS-AIME,* 1963, vol. 227, p. 1426.
13. J. M. Chilton, C. J. Barton, and G. R. Speich, *J. Iron Steel Inst.,* 1970, vol. 208, p. 184.
14. J. C. M. Li: *Trans. TMS-AIME,* 1963, vol. 227, p. 239.
15. S. Floreen: *Trans. TMS-AIME,* 1964, vol. 230, p. 842.
16. W. B. Morrison and R. L. Miller: Proc. of the 16th Sagamore Conference, Raquette Lake, N. Y., 1969.
17. Z. S. Basinski and P. J. Jackson: *Appl. Phys. Lett.*, 1945, vol. 6, p. 148.
18. J. H. Hollomon: *Trans. TMS-AIME,* 1945, vol. 162, p. 268.
19. J. Tanaka, C. A. Pampillo, and J. R. Low: ASTM Spec. Tech. Publ. No. 463, 1970.
20. See J. R. Low, Jr.: *Eng. Fract. Mech.* 1968, vol. 1, p. 47.